Published in final edited form as:
J Hepatol. 2012 October ; 57(4): 752–758. doi:10.1016/j.jhep.2012.05.014.

The Role of CX_3CL1/CX_3CR1 in Pulmonary Angiogenesis and Intravascular Monocyte Accumulation in Rat Experimental Hepatopulmonary Syndrome

Junlan Zhang[1], **Wenli Yang**[1], **Bao Luo**[1], **Bingqian Hu**[1], **Akhil Maheshwari**[2], and **Michael B. Fallon**[1]

[1] Department of Internal Medicine, Division of Gastroenterology, Hepatology and Nutrition, The University of Texas Health Science Center at Houston.

[2] Division of Neonatology, University of Illinois at Chicago

Abstract

Background & Aims—Hepatopulmonary syndrome (HPS), classically attributed to intrapulmonary vascular dilatation, occurs in 15-30% of cirrhotics and causes hypoxemia and increased mortality. In experimental HPS after common bile duct ligation (CBDL), monocytes adhere in the lung vasculature and produce vascular endothelial growth factor (VEGF)-A and angiogenesis ensues and contributes to abnormal gas exchange. However, the mechanisms for these events are unknown. The chemokine fractalkine (CX_3CL1) can directly mediate monocyte adhesion and activate VEGF-A and angiogenesis via its receptor CX_3CR1 on monocytes and endothelium during inflammatory angiogenesis. We explored whether pulmonary CX_3CL1/CX_3CR1 alterations occur after CBDL and influence pulmonary angiogenesis and HPS.

Methods—Pulmonary CX_3CL1/CX_3CR1 expression and localization, CX_3CL1 signaling pathway activation, monocyte accumulation, and the development of angiogenesis and HPS were assessed in 2 and 4wk CBDL animals. The effects of a neutralizing antibody to CX_3CR1 (anti-CX_3CR1 Ab) on HPS after CBDL were evaluated.

Results—Circulating CX_3CL1 levels and lung expression of CX_3CL1 and CX_3CR1 in intravascular monocytes and microvascular endothelium increased in 2 and 4wk CBDL animals as HPS developed. These events were accompanied by pulmonary angiogenesis, monocyte accumulation, activation of CX_3CL1 mediated signaling pathways (Akt, ERK) and increased VEGF-A expression and signaling. Anti-CX_3CR1 Ab treatment reduced monocyte accumulation, decreased lung angiogenesis and improved HPS. These events were accompanied by inhibition of CX_3CL1 signaling pathways and a reduction in VEGF-A expression and signaling.

Conclusions—Circulating CX_3CL1 levels and pulmonary CX_3CL1/CX_3CR1 expression and signaling increase after CBDL and contribute to pulmonary intravascular monocyte accumulation, angiogenesis and the development of experimental HPS.

Keywords

hepatopulmonary syndrome; common bile duct ligation; angiogenesis; fractalkine

Correspondence & contact information: Michael B. Fallon, MD The University of Texas Health Science Center at Houston UT Medical School Houston, Department of Internal Medicine Division of Gastroenterology, Hepatology and Nutrition 6431 Fannin Street, MSB 4.234 Houston, TX 77030-1501 Phone: 713.500.6677 Fax: 713.500.6699.

The authors declared that they do not have anything to disclose regarding conflict of interest with respect to this manuscript. The funding sources had no role in preparation of the manuscript.

Introduction

The hepatopulmonary syndrome (HPS) occurs when pulmonary microvascular alterations impair arterial oxygenation, in 15–30% of patients with cirrhosis. Its presence significantly increases mortality [1-4] and no effective medical therapies are available. Chronic common bile duct ligation (CBDL) in the rat is a model system for the study of HPS. In prior studies, we and others have observed that pulmonary angiogenesis occurs in CBDL animals as experimental HPS develops [5, 6]. This process is contributed by monocyte accumulation and vascular endothelial growth factor-A (VEGF-A) production and signaling in the pulmonary microvasculature, as well as activation of Akt and endothelial nitric oxide synthase (eNOS) in the pulmonary endothelium [5]. However, the mechanisms involved in monocyte accumulation and activation of angiogenic signaling after CBDL are undefined.

The observation that circulating monocytes are recruited to specific vascular regions and play a central role in angiogenesis has been made in a number of pathologic situations, including cutaneous wound healing/inflammatory angiogenesis [7, 8] and tumor angiogenesis [9, 10]. The homing of monocytes to areas of wound/inflammation or to tumors requires elaboration of specific chemokines, or leukocyte chemoattractant proteins categorized in to four groups based on conserved cysteine residues; C, CC, CXC and CX_3C and each has a specific cognate receptor through which signaling occurs [7, 10, 11]. The major chemokine/chemokine receptor pairs implicated in monocyte recruitment to the vasculature include monocyte chemotactic protein-1 (MCP-1)/CCL2-CCR2, macrophage inflammatory protein-1 alpha (MIP-1α)/CCL3-CCR1, stromal derived factor-1 alpha (SDF-1α)/CXCL12-CXCR4, RANTES/CCL5-CCR5 and fractalkine/CX_3CL1-CX_3CR1 [11-13]. Circulating soluble CX_3CL1 levels and biliary expression of CX_3CL1 are increased in cholestatic liver disease [14, 15] and binding of membrane bound CX_3CL1 to the CX_3CR1 receptor on monocytes results in rapid and firm arrest under physiologic conditions [16]. In addition, CX_3CL1 signaling has been implicated in both monocyte VEGF-A production and direct activation of Raf/MEK/ERK and PI3K/Akt/eNOS angiogenic signaling in endothelium [12, 17]. These findings raise the possibility that altered CX_3CL1/CX_3CR1 expression and signaling could play a role in monocyte accumulation and angiogenesis in experimental HPS.

Therefore, our aim was to define if pulmonary CX_3CL1 and CX_3CR1 expression and signaling are altered after CBDL and influence monocyte accumulation, angiogenic signaling pathways and the development of HPS. To address this aim, we assessed lung CX_3CL1 and CX_3CR1 expression, localization and signaling and evaluated the effects of anti-CX_3CR1 Ab administration after CBDL in relation to the development of lung angiogenesis and HPS.

Materials and Methods

Animals

Male Sprague-Dawley rats (200-250 g; Charles River, Wilmington, MA) were used in all experiments. CBDL was performed as described [18]. Control animals underwent mobilization of the common bile duct without ligation. In the 2 week CBDL protocol, rats were intraperitoneally injected with rabbit anti-CX_3CR1-neutralizing polyclonal antibody or normal rabbit IgG (anti-CX_3CR1 Ab or control IgG, 80 μg/kg body weight each day for 6 days, Torrey Pines Biolabs, East Orange, NJ) beginning 1 week after CBDL and analysis performed at 2 weeks [7]. In the 4 week CBDL protocol, anti-CX_3CR1 Ab or control IgG were given to animals for two weeks beginning 2 weeks after CBDL and analysis performed at 4 weeks. 5 to 8 animals from each group were used. Lung tissues and plasma were obtained from each animal. All animals had measurements of plasma bilirubin levels, portal

venous pressure and spleen weight [18-20]. The study was approved by The University of Texas at Houston Health Science Center Animal Welfare Committee and conformed to National Institutes of Health guidelines on the use of laboratory animals.

Measurement of Plasma CX_3CL1 Levels

Plasma soluble CX_3CL1 concentrations were measured with a specific enzyme-linked immuneabsorbent assay using capture and detection CX_3CL1 antibodies from R&D Systems, Inc. (Minneapolis, MN). The intensity of the color was measured in a microplate reader (Molecular Devices, Sunnyvale, CA).

RNA Extraction and quantitative real-time RT-PCR

Total RNA from lung was extracted with Trizol (Invitrogen, Carlsbad, CA) reagent according to the manufacturer's instructions and treated with RNase-free DNase I (Invitrogen) following the manufacturer's protocol. 2 μg of total RNA from lung was reverse transcribed into cDNA using the StrataScript first-strand synthesis system (Stratagene, La Jolla, CA). CX_3CL1 (sense: 5'-CTGCTGGCTGGTTAGAGG-3', anti-sense: GCTGCTGCTTGTAAGATGG-3') and CX_3CR1 (sense: 5'-GGTTGTTGTCTTCTTCCTCTTCTG-3', anti-sense: 5'-CGCCACTGTCTCCGTCAC-3') were amplified using SYBR Green PCR master mix (Applied Biosystems, Foster City, CA) and iCycler real-time PCR detection system (Bio-Rad) for 40 cycles. Relative levels were calculated using the iCycler software and a standard equation (Applied Biosystems) and normalized to GAPDH (sense: 5'-CCTGGTATGACAATGAATATG-3', anti-sense: 5'-TCTCTTGCTCTCAGTATCC-3').

Immunofluorescent and Immunohistochemical Localization

Five μm sections of 4% paraformaldehyde paraffin fixed lung tissues were blocked and incubated with primary antibodies. For immunofluorescent staining for CX_3CL1 (eBioscience, San Diego, CA), Texas red secondary antibody (Vector Laboratories, Burlingame, CA) and mounting medium with DAPI (Vector) were used. For immunofluorescent double-labeling for CX_3CR1 (eBioscience) with ED1 (Serotec, Raleigh, NC), factor VIII (FVIII, Cell Marque, Austin, TX) with ED1 or VEGF-A (Santa Cruz, Biotechnology, Santa Cruz, CA) with ED1, after using Texas red secondary antibody, the initial incubation were followed by second primary antibody application, washing, secondary antibody incubation using fluorescent secondary antibodies (Vector). Sections are photographed with an Axiophot microscope (Nikon, Melville, NY). Controls are incubated with secondary antibody alone.

Arterial Blood Gas Analysis

Arterial blood was drawn from the femoral artery as previously described [18, 19] and blood gas analysis was performed on an ABL 520 radiometer (Radiometer America, Westlake, OH). The alveolar–arterial oxygen gradient was calculated as $150 - (PaCO_2/0.8) - PaO_2$.

Microvascular Density and Quantitation

The degree of pulmonary angiogenesis was quantified by microvessel density in lung sections obtained from one entire lobe for each animal and immunostained with endothelial marker Factor VIII. All stained objects were counted in a blinded fashion. Vessels with thick muscular walls or larger than 100 μm in diameter were excluded. All the scanned fields of three to five sections from each animal were investigated. The average microvessel count per square millimeter after CBDL was expressed relative to the count of control as fold control values [5].

Western Blot Analysis

Lung tissues were homogenized in radioimmunoprecipitation buffer in the presence of protease inhibitors, as previously described [20]. Equal concentrations of protein from lung were fractionated on Tris-HCl–ready gels (Bio-Rad Laboratories, Hercules, CA) and transferred to nitrocellulose membranes (Bio-Rad). Incubation with primary antibodies for von Willebrand factor (vWf), PCNA, VEGF-A, vascular endothelial growth factor receptor-2 (VEGFR-2, Santa Cruz), Akt, phospho-Akt (p-Akt, Ser473), phospho-vascular endothelial growth factor receptor-2 (p-VEGFR-2, Tyr1175), ERK, phospho-ERK (p-ERK, Thr202/Tyr204, Cell Signaling, Danvers, MA) or ED1 was followed by the addition of horseradish peroxidase-conjugated secondary antibodies and detection with enhanced chemiluminescence. The density of autoradiographic signals was assessed with a ScanMaker i900 scanner (Microtek Lab, Carson, CA) and quantitated with ImageJ software provided by National Institutes of Health.

Statistics

Data were analyzed with the Student *t* test or analysis of variance with Bonferroni correction for multiple comparisons between groups. Measurements are expressed as means ± SE. Statistical significance was designated as $P < 0.05$.

Results

Circulating CX_3CL1 Levels and Lung CX_3CL1/CX_3CR1 Expression and Localization after CBDL

To determine whether pulmonary chemokine/chemokine receptor alterations occur after CBDL, we measured the expression of fractalkine/CX_3CL1 (Fig.1) and its receptor CX_3CR1 (Fig.2) in the lung using real-time quantitative RT-PCR and immunohistochemical staining. We found an increase in lung expression of both CX_3CL1 (4.1 and 4.3 fold-control, Fig.1B) and CX_3CR1 (5.0 and 4.2 fold-control, Fig.2B) in 2wk and 4wk CBDL animals, respectively. These alterations were accompanied by a significant increase in circulating CX_3CL1 levels after CBDL (Fig.1C). To localize the increases in pulmonary CX_3CL1 and CX_3CR1 expression in response to CBDL, we performed immunoflourescence double-labeling for CX_3CL1 or CX_3CR1 with ED1, a specific monocyte marker. In normal lung, there was minimal monocyte (in line with prior studies) and CX_3CL1 staining. In 2wk CBDL animals, there was a substantial increase in CX_3CL1-positive staining found both in intravascular monocytes and pulmonary microvascular endothelial cells (Fig.1A). Pulmonary CX_3CR1 staining was present in the pulmonary microvasculature in normal animals. After 2wk CBDL, a marked increase in CX_3CR1 staining was observed, one component of which localized to intravascular monocytes and another to the microvasculature in a pattern consistent with endothelial cell staining (Fig.2A).

Effects of Neutralizing Anti-CX_3CR1 Antibody on the Development of Pulmonary Angiogenesis after CBDL

To explore whether altered pulmonary CX_3CL1 and CX_3CR1 expression modulates pulmonary angiogenesis, we assessed lung angiogenesis in the presence or absence of neutralizing anti-CX_3CR1 antibody during the initiation of HPS in 2 week CBDL animals. Angiogenesis was assessed by quantifying FVIII stained microvessels and by measuring vWf and PCNA levels as reported previously (Fig.3) [5]. Compared with control animals where basal FVIII staining in the pulmonary microvasculature was observed (Fig.3A), angiogenesis was seen at 2 weeks after CBDL reflected by a marked increase in FVIII microvessel staining and counts and by increased vWf and PCNA levels as reported previously (Fig.3B and 3C) [5]. Anti-CX_3CR1 Ab administration in 2wk CBDL animals

resulted in a significant reduction in pulmonary FVIII staining and microvessel counts and lung vWf and PCNA levels, indicating a significant inhibition of angiogenesis (Fig.3A – 3C).

Effects of Neutralizing Anti-CX_3CR1 Antibody on Pulmonary VEGF-A/VEGFR-2 activation and monocyte accumulation after CBDL

To define the mechanisms through which CX_3CL1/CX_3CR1 influence angiogenesis, we assessed VEGF signaling and intravascular monocyte accumulation after CBDL in the presence or absence of neutralizing anti-CX_3CR1 antibody (Fig.4). In control animals, where angiogenesis was absent, lung VEGF-A and ED1 staining was minimal as were the levels of VEGF-A, p-VEGFR-2 and ED1. In 2wk CBDL animals, there was a marked increase in VEGF-A staining, predominately co-localized with ED1 in intravascular monocytes, but also in a microvasculature pattern consistent with endothelial staining (Fig. 4A). These increases were accompanied by a significant rise in pulmonary VEGF-A and p-VEGFR-2 levels (Fig.4B and 4C) reflecting activation of VEGF signaling and by a significant increase in ED1 levels due to the influx of intravascular monocytes (Fig.4D) [5]. Anti-CX_3CR1 Ab treatment resulted in a specific decrease in intravascular monocyte accumulation based on ED1 staining and levels (Fig.4A and 4D) and a reduction in VEGF-A staining and levels and VEGFR-2 phosphorylation compared with untreated CBDL animals (Fig.4A – 4C).

Effects of Neutralizing Anti-CX_3CR1 Antibody on Pulmonary Akt and ERK Activation after CBDL

To assess whether CX_3CL1 mediated pro-angiogenic endothelial signaling pathways are activated after CBDL, we measured pulmonary p-Akt and p-ERK levels by Western blot analysis in 2 week CBDL animals with or without anti-CX_3CR1 Ab administration (Fig.4E and 4F). Pulmonary levels of both p-Akt and p-ERK increased significantly in 2wk CBDL animals [5, 21] and were substantially reduced by anti-CX_3CR1 Ab treatment.

Effects of Neutralizing Anti-CX_3CR1 Antibody on HPS and Portal Hypertension after CBDL

To directly define whether CX_3CL1/CX_3CR1 mediated events influence the development of experimental HPS, we measured pulmonary and hepatic alterations in 2 week CBDL animals in the presence or absence of neutralizing anti-CX_3CR1 antibody (Table 1). In 2wk CBDL animals with control antibody treatment, HPS developed, as reflected by a significant increase in the alveolar arterial oxygen gradient relative to controls and was accompanied by an increase in plasma bilirubin levels, portal venous pressure and spleen weight. Anti-CX_3CR1 Ab administration resulted in a significant improvement in alveolar–arterial oxygen gradient without influencing plasma bilirubin levels, portal venous pressure or spleen weight.

Effects of Neutralizing Anti-CX_3CR1 Antibody on Pulmonary Alterations in established HPS and cirrhosis after CBDL

To define whether inhibition of CX_3CR1 also modulates established gas exchange abnormalities and pulmonary events of HPS in animals with cirrhosis, we administered anti-CX_3CR1 Ab or control IgG to CBDL animals beginning at 2 weeks after surgery for 2 weeks and evaluated these animals at 4 weeks after CBDL (Fig.5). Control IgG treated CBDL animals had elevated portal venous pressures (17.0 ± 2.0 mmHg), moderately higher than 2 week animals, and similar to prior results [22]. Anti-CX_3CR1 Ab treatment did not influence portal pressures in 4 week CBDL animals (18.3 ± 1.9 mmHg). Moreover, control IgG treated CBDL animal developed impaired alveolar–arterial oxygen gradients (Fig.5A), and pulmonary alterations of HPS characterized by increases in lung vessel density (Fig.5B)

and monocyte accumulation (ED1 levels) and activation of Akt and ERK signaling (Fig.5C). Each of these events were attenuated by anti-CX_3CR1 Ab treatment in CBDL animals indicating that inhibition of the CX_3CL1/CX_3CR1 pathway influences established HPS in the setting of cirrhosis (Fig.5A-5C).

Discussion

In prior studies, we found and others have confirmed that accumulation of intravascular monocytes and production of VEGF-A in the lung vasculature triggers angiogenesis and contributes to abnormal gas exchange in experimental HPS [5]. A number of angiogenic conditions are associated with monocyte accumulation and the angiogenic process is controlled by a variety of positive and negative regulators, including growth factors, cytokines, adhesion molecules and chemokines [23]. In this study, we focused on the novel concept that chemokine alterations resulting from liver disease may contribute to the development of extrahepatic complications. Specifically, we focused on the chemokine/chemokine receptor pair fractalkine/CX_3CL1-CX_3CR1 based on the recognition that expression may be altered in liver disease and the ability of the receptor-ligand interaction to induce firm monocyte adhesion and directly activate angiogenesis [12, 13, 24]. We found that lung CX_3CL1 and CX_3CR1 expression increased in intravascular monocytes and microvascular endothelial regions and was associated with increased circulating CX_3CL1 levels in CBDL animals. These changes were accompanied by pulmonary angiogenesis, activation of CX_3CL1/CX_3CR1 mediated angiogenic signaling pathways and the development of HPS. Further, blockade of CX_3CR1 activation both during the development of HPS and in established HPS and cirrhosis decreases monocyte accumulation and improves angiogenesis and HPS. Together, these findings provide direct evidence that altered chemokine expression and function contribute to experimental HPS and identify CX_3CL1/CX_3CR1 as one relevant contributor.

Common bile duct ligation is the only established experimental model of human HPS. The development of HPS in experimental models and in humans does not require advanced and long-standing liver disease [1, 25-28]. In animals, biliary type liver injury begins shortly after CBDL [22, 29] and within two weeks, bridging fibrosis, portal hypertension, a hyperdynamic circulation and HPS develop [18, 20, 22]. The hyperdynamic and liver changes generally progress over the course of CBDL, although changes in mean arterial pressure and portal venous pressure do not reach statistical significance between 2-week CBDL animals and those at 4 weeks when cirrhosis is fully established [22]. We have also found that all animals with complete biliary obstruction develop HPS [18]. Therefore, animals where complete obstruction does not develop due to recanalization [30-32] are excluded from analysis based on biochemical, histologic and hemodynamic parameters. In the current study, we specifically chose to evaluate animals early in the sequence of events that lead to HPS (between 1 and 2 weeks after CBDL) so that we could define the effects of inhibition of CX_3CR1 signaling on the development of HPS. In addition, to determine whether CX3CL1/CX3CR1 pathway remains an important contributor to the pulmonary alterations when HPS and cirrhosis are well established, we also evaluated the effects of CX3CR1 blockade (beginning at two weeks after CBDL) on pulmonary abnormalities of HPS in animals after 4wk CBDL.

CX_3CL1 is expressed as a transmembrane protein on the plasma membrane and may be subsequently cleaved by proteases resulting in a soluble agonist. The membrane form mediates cell-cell adhesion by binding CX_3CR1 on adjacent cells whereas both the soluble and membrane forms of CX_3CL1 may mediate chemotactic and angiogenic responses by activating CX_3CR1 in relevant cell types [12, 33, 34]. Alterations in CX_3CL1/CX_3CR1 have been found in a number of conditions affecting liver and lung[14, 15, 35, 36], and in several

of these conditions CX_3CL1/CX_3CR1 signaling contributes to monocyte accumulation and angiogenesis [7]. A variety of factors relevant to liver disease may influence CX_3CL1 expression (interferon-gamma, TNF-α, IL-1β, shear stress and endothelin-1) [37] and CX_3CR1 expression [38]. In addition, biliary epithelium has been identified as a source of circulating CX_3CL1 in experimental and human cholestatic injury [14, 15]. In the current work, we find an increase in circulating CX_3CL1 and in CX_3CL1 and CX_3CR1 expression in lung regions relevant for the development of HPS. These findings confirm that circulating CX_3CL1 levels are increased in cholestatic liver disease and suggest that lung CX_3CL1/CX_3CR1 expression may be altered by inflammatory mediators elaborated during liver injury. However, which inflammatory mediators are involved, whether the changes in CX_3CL1/CX_3CR1 are unique to the lung and whether differences in inflammatory mediators produced explain the unique development of HPS in CBDL animals relative to other cirrhosis models are areas for further study.

The increase in circulating CX_3CL1 and in CX_3CL1/CX_3CR1 expression in the lung microvascular endothelium and in intravascular monocytes after CBDL is accompanied by accumulation of monocytes, pulmonary angiogenesis and the onset of HPS. Moreover, the inhibition of CX_3CR1 signaling decreases intravascular monocyte accumulation, reduces pulmonary angiogenesis and improves HPS. These results are in line with prior studies in skin where activation of CX_3CL1/CX_3CR1 triggers monocyte accumulation and angiogenesis during wound healing [7] and in hind limb ischemia where CX_3CL1/CX_3CR1 activation in vascular endothelium leads to an angiogenic response [17]. Taken together, these results implicate CX_3CL1/CX_3CR1 activation in monocyte accumulation and angiogenesis in experimental HPS. Interestingly, in the current work CX_3CR1 inhibition did not influence the degree of portal hypertension or hepatic injury after CBDL. This finding supports that the development of liver injury and portal hypertension likely involve multiple pathways and/or that the duration and timing of CX_3CR1 inhibition in the current study may have been insufficient to modulate CX_3CL1/CX_3CR1 effects in the liver.

We also explored the mechanisms through which CX_3CL1/CX_3CR1 contribute to angiogenesis in experimental HPS. In prior studies, CX_3CR1 mediated angiogenesis has been established to occur through increased VEGF-A expression, activation of VEGFA/VEGFR-2 signaling and the induction of two major signaling cascades that regulate endothelial cell proliferation, migration and survival, the phosphatidylinositol 3-kinase /Akt and Raf/MEK/ERK pathways [39-45]. In our previous CBDL studies, we found that pulmonary intravascular monocytes produce a number of factors that may influence angiogenesis including nitric oxide, carbon monoxide and VEGF-A and that lung Akt activation occurs as HPS develops [22, 46]. In the current study, CX_3CR1 inhibition blocked monocyte accumulation and reduced VEGF-A production and activation of VEGF-A dependent signaling pathways. These results support that one important mechanism for CX_3CL1 effects on angiogenesis and HPS is modulation of monocyte adhesion and VEGF-A levels in the pulmonary microvasculature. We also found that lung Akt and ERK pathways are activated after CBDL as angiogenesis develops and are down regulated by CX_3CR1 inhibition as HPS improves. This finding suggests that CX_3CL1 directly activates key angiogenic pathways in the pulmonary endothelium that contribute to experimental HPS.

In summary, our work shows that increased circulating CX_3CL1 levels and an increase in CX_3CL1/CX_3CR1 production in intravascular monocytes and the pulmonary microvasculature are found during the development of pulmonary angiogenesis and contribute to HPS in CBDL animals. This process involves the adherence of monocytes in the pulmonary microvasculature with subsequent production of VEGF-A and activation of Akt and ERK in the lung. Together these findings provide direct support for the concept that

chemokine alterations in liver disease may play an important role in the development of extrahepatic complications of cirrhosis. Although additional factors likely contribute to the development of experimental HPS after CBDL, our findings provide a novel conceptual framework for understanding the mechanisms and designing treatments for HPS and possibly other complications of cirrhosis.

Acknowledgments

Supported by 5DKR01DK056804 to M.B.F, and a Scientist Development Award (AHA) and a Pilot/Feasibility project (The Texas Medical Center Digestive Diseases Center) to J.Z.

Abbreviations used in this paper

HPS	hepatopulmonary Syndrome
CBDL	common bile duct ligation
VEGF	vascular endothelial growth factor
eNOS	endothelial nitric oxide synthase
MCP-1	monocyte chemotactic protein-1
MIP-1α	macrophage inflammatory protein-1 alpha
SDF-1α	stromal derived factor-1 alpha
RANTES	regulated upon activation, normal T cell expressed and secreted
anti-CX_3CR1 Ab	anti-CX_3CR1-neutralizing antibody
ERK	extracellular signal-regulated kinase
FVIII	factor VIII
vWf	von Willebrand factor
MEK	mitogen-activated protein kinase kinase
p-Akt	phospho-Akt
PCNA	proliferating cell nuclear antigen
p-VEGFR-2	phospho-vascular endothelial growth factor receptor-2

References

1. Rodriguez-Roisin R, Krowka MJ. Hepatopulmonary syndrome -- a liver-induced lung vascular disorder. N Engl J Med. 2008; 358:2378–2387. [PubMed: 18509123]
2. Fallon MB, Krowka MJ, Brown RS, Trotter JF, Zacks S, Roberts KE, et al. Impact of hepatopulmonary syndrome on quality of life and survival in liver transplant candidates. Gastroenterology. 2008; 135:1168–1175. [PubMed: 18644373]
3. Schenk P, Schoniger-Hekele M, Fuhrmann V, Madl C, Silberhumer G, Muller C. Prognostic significance of the hepatopulmonary syndrome in patients with cirrhosis. Gastroenterology. 2003; 125:1042–1052. [PubMed: 14517788]
4. Swanson K, Wiesner R, Krowka M. Natural history of hepatopulmonary syndrome: Impact of liver transplantation. Hepatology. 2005; 41:1122–1129. [PubMed: 15828054]
5. Zhang J, Luo B, Tang L, Wang Y, Stockard CR, Kadish I, et al. Pulmonary angiogenesis in a rat model of hepatopulmonary syndrome. Gastroenterology. 2009; 136:1070–1080. [PubMed: 19109954]

6. Thenappan T, Goel A, Marsboom G, Fang Y-H, Toth PT, Zhang HJ, et al. A central role for cd68(+) macrophages in hepatopulmonary syndrome: Reversal by macrophage depletion. Am J Respir Crit Care Med. 183:1080–1091. [PubMed: 21148721]
7. Ishida Y, Gao J-L, Murphy PM. Chemokine receptor cx3cr1 mediates skin wound healing by promoting macrophage and fibroblast accumulation and function. J Immunol. 2008; 180:569–579. [PubMed: 18097059]
8. Szekanecz Z, Koch A. Macrophages and their products in rheumatoid arthritis. Curr Opin Rheumatol. 2007; 19:289–295. [PubMed: 17414958]
9. De Palma M, Murdoch C, Venneri MA, Naldini L, Lewis CE. Tie2-expressing monocytes: Regulation of tumor angiogenesis and therapeutic implications. Trends Immunol. 2007; 28:545–550.
10. Schmid MC, Varner JA. Myeloid cell trafficking and tumor angiogenesis. Cancer Letters. 2007; 250:1–8. [PubMed: 17049723]
11. Gillitzer R, Goebeler M. Chemokines in cutaneous wound healing. J Leukoc Biol. 2001; 69:513–521. [PubMed: 11310836]
12. Lee S-J, Namkoong S, Kim Y-M, Kim C-K, Lee H, Ha K-S, et al. Fractalkine stimulates angiogenesis by activating the raf-1/mek/erk- and pi3k/akt/enos-dependent signal pathways. Am J Physiol Heart Circ Physiol. 2006; 291:H2836–2846. [PubMed: 16877565]
13. Stellos KMD, Gawaz MMD. Platelets and stromal cell-derived factor-1 in progenitor cell recruitment. Semin Thromb Hemost. 2007:159–164. [PubMed: 17340464]
14. Efsen E, Grappone C, DeFranco RMS, Milani S, Romanelli RG, Bonacchi A, et al. Up-regulated expression of fractalkine and its receptor cx3cr1 during liver injury in humans. Journal of Hepatology. 2002; 37:39–47. [PubMed: 12076860]
15. Isse K, Harada K, Zen Y, Kamihira T, Shimoda S, Harada M, et al. Fractalkine and cx3cr1 are involved in the recruitment of intraepithelial lymphocytes of intrahepatic bile ducts. Hepatology. 2005; 41:506–516. [PubMed: 15726664]
16. Imai T, Hieshima K, Haskell C, Baba M, Nagira M, Nishimura M, et al. Identification and molecular characterization of fractalkine receptor cx3cr1, which mediates both leukocyte migration and adhesion. Cell. 1997; 91:521–530. [PubMed: 9390561]
17. Ryu J, Lee C-W, Hong K-H, Shin J-A, Lim S-H, Park C-S, et al. Activation of fractalkine/cx3cr1 by vascular endothelial cells induces angiogenesis through vegf-a/kdr and reverses hindlimb ischaemia. Cardiovasc Res. 2008; 78:333–340. [PubMed: 18006432]
18. Fallon MB, Abrams GA, McGrath JW, Hou Z, Luo B. Common bile duct ligation in the rat: A model of intrapulmonary vasodilatation and hepatopulmonary syndrome. Am J Physiol. 1997; 272:G779–G784. [PubMed: 9142908]
19. Fallon MB, Abrams GA, Luo B, Hou Z, Chen YF, Oparil S. Altered organ levels of vasoactive mediators in cirrhotic and non-cirrhotic rat models of portal hypertension. Gastroenterology. 1997; 112(4):A1262.
20. Fallon MB, Abrams GA, Luo B, Hou Z, Dai J, Ku DD. The role of endothelial nitric oxide synthase in the pathogenesis of a rat model of hepatopulmonary syndrome. Gastroenterology. 1997; 113:606–614. [PubMed: 9247483]
21. Tang L, Luo B, Patel RP, Ling Y, Zhang J, Fallon MB. Modulation of pulmonary endothelial endothelin b receptor expression and signaling: Implications for experimental hepatopulmonary syndrome. Am J Physiol Lung Cell Mol Physiol. 2007; 292:L1467–1472. [PubMed: 17337507]
22. Zhang J, Ling Y, Luo B, Tang L, Stockard C, Grizzle WE, et al. Analysis of pulmonary heme oxygenase-1 and nitric oxide synthase alterations in experimental hepatopulmonary syndrome. Gastroenterology. 2003; 125:1441–1451. [PubMed: 14598260]
23. Aalinkeel R, Nair MPN, Sufrin G, Mahajan SD, Chadha KC, Chawda RP, et al. Gene expression of angiogenic factors correlates with metastatic potential of prostate cancer cells. Cancer Res. 2004; 64:5311–5321. [PubMed: 15289337]
24. Xia Y, Frangogiannis N. Mcp-1/ccl2 as a therapeutic target in myocardial infarction and ischemic cardiomyopathy. Inflamm Allergy Drug Targets. 2007; 6:101–107. [PubMed: 17692033]

25. Teuber G, Teupe C, Dietrich C, Caspary W, Buhl R, Zeuzem S. Pulmonary dysfunction in non-cirrhotic patients with chronic viral hepatitis. Eur J Intern Med. 2002; 13:311–318. [PubMed: 12144910]
26. Gupta D, Vijaya DR, Gupta R, Dhiman RK, Bhargava M, Verma J, et al. Prevalence of hepatopulmonary syndrome in cirrhosis and extrahepatic portal venous obstruction. Am J Gastroenterol. 2001; 96:3395–3399. [PubMed: 11774955]
27. Regev A, Yeshurun M, Rodriguez M, Sagie A, Neff G, Molina E, et al. Transient hepatopulmonary syndrome in a patient with acute hepatitis a. J Viral Hep. 2001; 8:83–86.
28. Rodriguez-Roisin R, Krowka MJ, Herve P, Fallon MB. on behalf of the ERS Task Force Pulmonary-Hepatic Vascular Disorders Scientific Committee ERS Task Force PHD Scientific Committee. Pulmonary-hepatic vascular disorders (phd). Eur Respir J. 2004; 24:861–880. [PubMed: 15516683]
29. Georgiev P, Jochum W, Heinrich S, Jang JH, Nocito A, Dahm F, et al. Characterization of time-related changes after experimental bile duct ligation. Br J Surg. 2008; 95:646–656. [PubMed: 18196571]
30. Aller MA, Nava MP, Arias JL, DurÃ¡n M, Prieto I, Llamas MA, et al. Microsurgical extrahepatic cholestasis in the rat: A long-term study. Journal of Investigative Surgery. 2004; 17:99–104. [PubMed: 15204716]
31. Holmberg JT, Hederstroum E, Ihse I. A method to prevent recanalization of the transected bile duct in the rat. Scandinavian Journal of Gastroenterology. 1985; 20:428–432. [PubMed: 4023608]
32. Wright JE, Braithwaite JL. The effects of ligation of the common bile duct in the rat. J Anat. 1964; 98:227–233. [PubMed: 14154425]
33. Ruth JH, Volin MV III GKH, Woodruff DC, Jr. KJK, Woods JM, et al. Fractalkine, a novel chemokine in rheumatoid arthritis and in rat adjuvant-induced arthritis. Arthritis & Rheumatism. 2001; 44:1568–1581. [PubMed: 11465708]
34. Volin MV, Woods JM, Amin MA, Connors MA, Harlow LA, Koch AE. Fractalkine: A novel angiogenic chemokine in rheumatoid arthritis. Am J Pathol. 2001; 159:1521–1530. [PubMed: 11583978]
35. Ars C, Thurion P, Delos M, Sibille Y, Pilette C. Small airway obstruction in severe pulmonary arterial hypertension correlates with increased airway cd8+ t-cells and fractalkine expression. Eur Respir J. 2009; 34:1494–1496. [PubMed: 19948918]
36. McComb JG, Ranganathan M, Liu XH, Pilewski JM, Ray P, Watkins SC, et al. Cx3cl1 up-regulation is associated with recruitment of cx3cr1+ mononuclear phagocytes and t lymphocytes in the lungs during cigarette smoke-induced emphysema. Am J Pathol. 2008; 173:949–961. [PubMed: 18772344]
37. Imaizumi T, Yoshida H, Satoh K. Regulation of cx3cl1/fractalkine expression in endothelial cells. J Atheroscler Thromb. 2004; 11:15–21. [PubMed: 15067194]
38. Stievano L, Piovan E, Amadori A. C and cx3c chemokines: Cell sources and physiopathological implications. Crit Rev Immunol. 2004; 24:205–228. [PubMed: 15482255]
39. Yu Y, Sato JD. Map kinases, phosphatidylinositol 3-kinase, and p70 s6 kinase mediate the mitogenic response of human endothelial cells to vascular endothelial growth factor. Journal of Cellular Physiology. 1999; 178:235–246. [PubMed: 10048588]
40. Gerber H-P, McMurtrey A, Kowalski J, Yan M, Keyt BA, Dixit V, et al. Vascular endothelial growth factor regulates endothelial cell survival through the phosphatidylinositol 3'-kinase/akt signal transduction pathway. Requirement for flk-1/kdr activation. J Biol Chem. 1998; 273:30336–30343. [PubMed: 9804796]
41. Gupta K, Kshirsagar S, Li W, Gui L, Ramakrishnan S, Gupta P, et al. Vegf prevents apoptosis of human microvascular endothelial cells via opposing effects on mapk/erk and sapk/jnk signaling. Experimental Cell Research. 1999; 247:495–504. [PubMed: 10066377]
42. Kroll J, Waltenberger J. The vascular endothelial growth factor receptor kdr activates multiple signal transduction pathways in porcine aortic endothelial cells. J Biol Chem. 1997; 272:32521–32527. [PubMed: 9405464]

43. Berra E, Milanini J, Richard DE, Le Gall M, Viñals F, Gothié E, et al. Signaling angiogenesis via p42/p44 map kinase and hypoxia. Biochemical Pharmacology. 2000; 60:1171–1178. [PubMed: 11007955]

44. Bullard LE, Qi X, Penn JS. Role for extracellular signal-responsive kinase-1 and -2 in retinal angiogenesis. Invest Ophthalmol Vis Sci. 2003; 44:1722–1731. [PubMed: 12657614]

45. Jiang B-H, Zheng JZ, Aoki M, Vogt PK. Phosphatidylinositol 3-kinase signaling mediates angiogenesis and expression of vascular endothelial growth factor in endothelial cells. Proceedings of the National Academy of Sciences of the United States of America. 2000; 97:1749–1753. [PubMed: 10677529]

46. Arguedas MR, Drake BB, Kapoor A, Fallon MB. Carboxyhemoglobin levels in cirrhotic patients with and without hepatopulmonary syndrome. Gastroenterology. 2005; 128:328–333. [PubMed: 15685544]

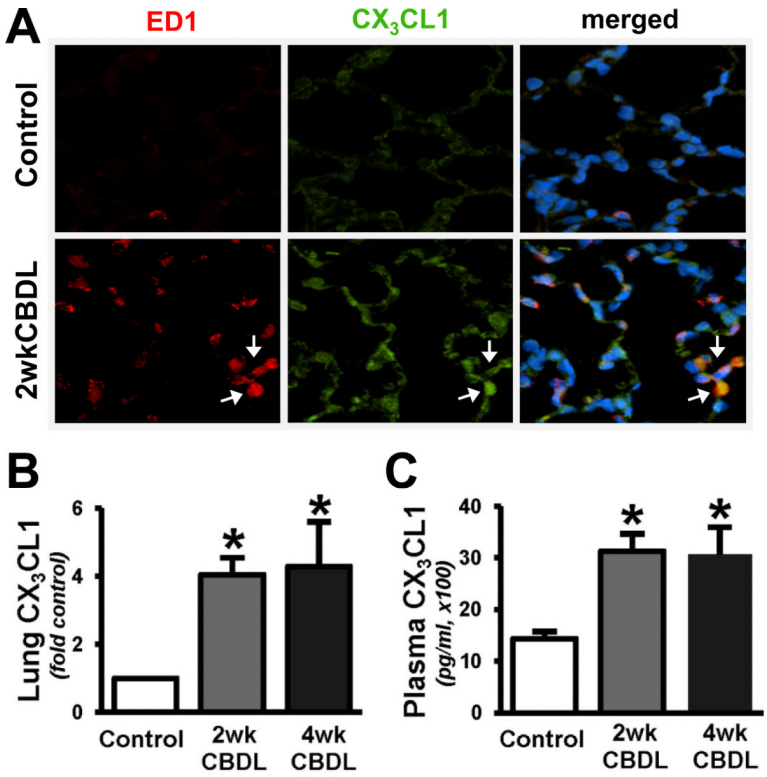

Fig. 1. Pulmonary fractalkine/CX_3CL1 expression and immunofluorescent localization, and plasma levels after CBDL

(A), representative double-labeling images of CX_3CL1 (green) and ED1 (red, a specific monocyte marker) and superimposition with DAPI (blue) in control and 2wk CBDL animals (shown by arrows, original magnification, 40×). The graphical summaries are shown of **(B)** CX_3CL1 mRNA levels in lungs and **(C)** circulating levels in plasma after 2wk (n=5) and 4wk CBDL (n=6) relative to control (n=6). Values are expressed as means ± SE. *$P < 0.05$ compared with control.

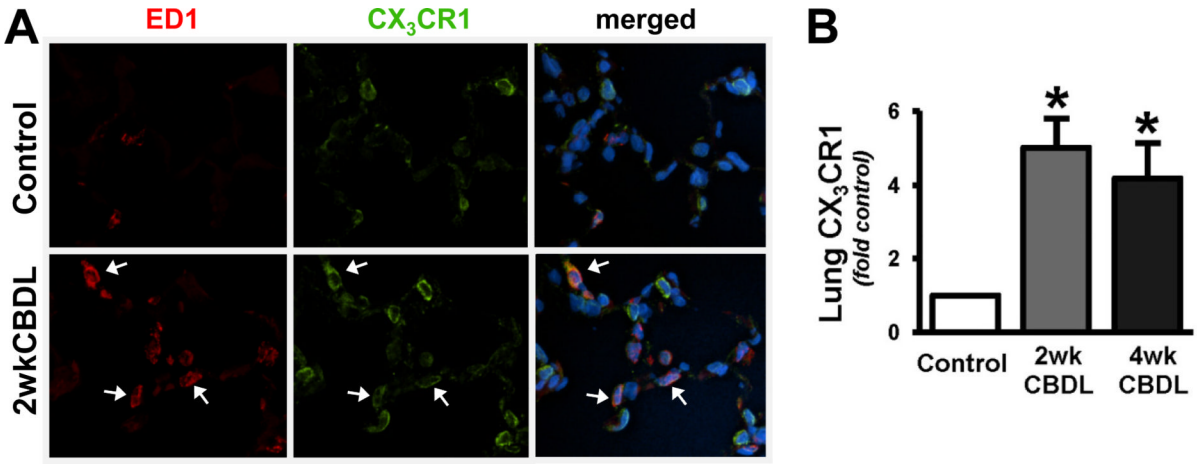

Fig. 2. Pulmonary CX_3CR1 expression and immunofluorescent localization after CBDL

(A), Representative double-labeling images of CX_3CR1 (green) and ED1 (red, a specific monocyte marker) and superimposition with DAPI (blue) in control and 2wk CBDL animals (show by arrows, original magnification 40×). **(B)**, the graphical summary of CX_3CR1 mRNA levels in lungs after 2wk (n=5) and 4wk CBDL (n=6) relative to control (n=6). Values are expressed as means ± SE. $*P < 0.05$ compared with control.

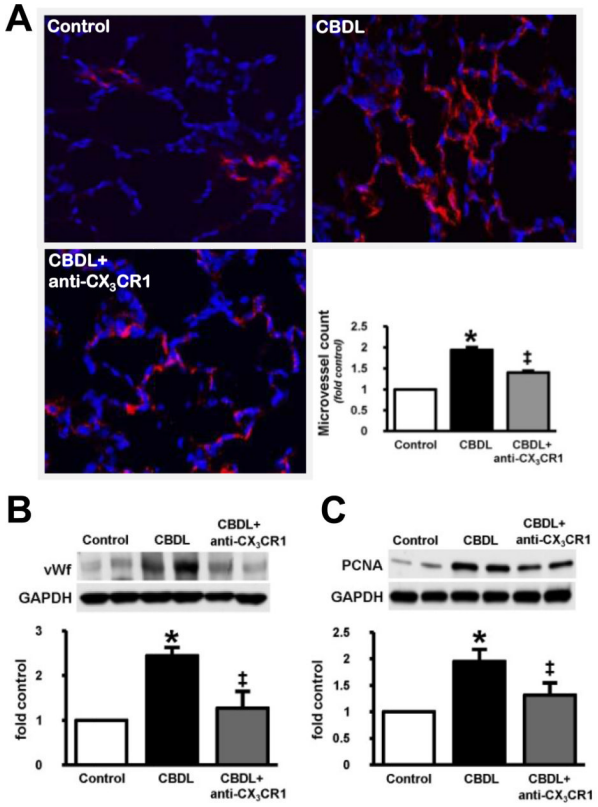

Fig. 3. Effect of CX_3CR1 neutralization on pulmonary FVIII immunostaining, microvessel counts and von Willebrand factor (vWf) and PCNA levels in 2wk CBDL animals

(A), immunostaining of FVIII (red) with blue DAPI nuclear stain (blue) in control, CBDLand anti-CX_3CR1-neutralizing antibody (anti-CX_3CR1 Ab) administered CBDL animals (original magnification, 40×) and the graphical summary of lung microvessel counts in all animal groups. The representative immunoblots and graphical summaries of **(B)** vWf and **(C)** PCNA levels in control (n=6), CBDL (n=5) and anti-CX_3CR1 Ab treated CBDL (n=8) animals are shown. Values are expressed as means ± SE. $^{*}P < 0.05$ compared with control. $^{‡}P < 0.05$ compared with CBDL.

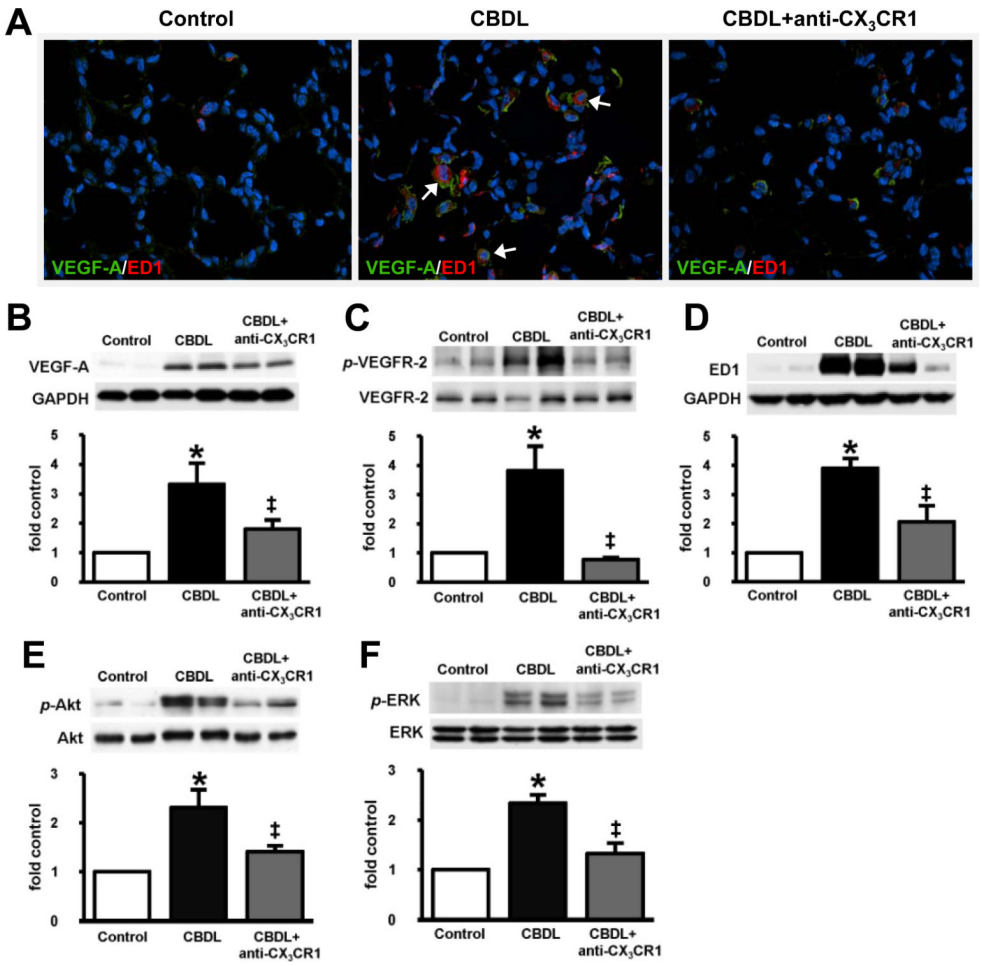

Fig. 4. Effect of CX_3CR1 neutralization on immunofluorescent localization and protein levels of lung VEGF-A, VEGFR-2 phosphorylation, monocyte accumulation and phosphorylation of Akt and ERK in 2wk CBDL animals

(A), representative double-labeling images of VEGF-A (green) and ED1 (red) with blue DAPI nuclear stain (blue) in control, CBDL and anti-CX_3CR1 Ab administered CBDL animals (shown by arrows, original magnification 40×). The representative immunoblots and graphical summaries of protein levels for **(B)** VEGF-A, **(C)** p-VEGFR-2, **(D)** ED1, **(E)** p-Akt/Akt and **(F)** p-ERK/ERK in control (n=6), CBDL (n=5) and anti-CX_3CR1 Ab treated CBDL (n=8) animals are shown. Values are expressed as means ± SE. $^{*}P < 0.05$ compared with control. $^{‡}P < 0.05$ compared with CBDL.

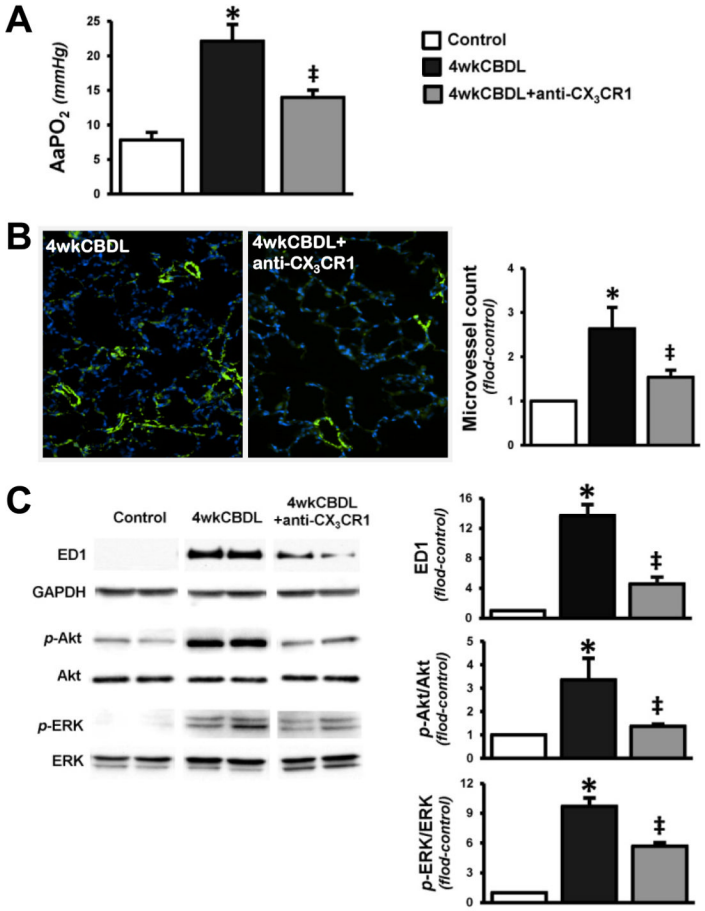

Fig. 5. Effect of CX_3CR1 neutralization on alveolar–arterial oxygen gradients, lung microvessel counts, monocytes accumulation and phosphorylation of Akt and ERK in 4wk CBDL animals

(A), the summaries of $AaPO_2$ in control, CBDL and anti-CX_3CR1 Ab administered CBDL animals. **(B)**, immunostaining of FVIII (green) with DAPI nuclear stain (blue) in CBDL and anti-CX_3CR1 Ab administered CBDL animals (original magnification, 20×) and the graphical summary of lung microvessel counts in all animal groups. **(C)**, the representative immunoblots and graphical summaries of protein levels for ED1, p-Akt/Akt and p-ERK/ERK in control (n=5), CBDL (n=6) and anti-CX_3CR1 Ab treated CBDL (n=6) animals. Values are expressed as means ± SE. $*P < 0.05$ compared with control. $‡P < 0.05$ compared with CBDL.

Table 1

Effect of CX_3CR1 neutralization on pulmonary and hepatic alterations in 2wk CBDL animals.

	Control (n=6)	CBDL (n=5)	CBDL + anti-CX_3CR1 Ab (n=8)
$AaPO_2$ (mmHg)	5.6 ± 1.5	14.5 ± 0.6 *	9.9 ± 1.9 ≠
PO_2 (mmHg)	94.5 ± 1.0	85.9 ± 0.8 *	94.3 ± 1.5 ≠
PCO_2 (mmHg)	38.5 ± 0.6	36.3 ± 1.1 *	36.4 ± 0.8 *
Bilirubin (mg/dl)	0.4 ± 0.1	8.7 ± 1.0 *	9.9 ± 0.9 *
PVP (mmHg)	7.2 ± 0.3	14.0 ± 0.6 *	12.8 ± 0.9 *
Spleen weight (g)	0.7 ± 0.1	1.3 ± 0.1 *	1.2 ± 0.1 *

Values are means ± SE. $AaPO_2$, alveolar-arterial oxygen gradient; CBDL, common bile duct ligation; PVP, portal venous pressure.

* $P < 0.05$ compared with control.

≠ $P < 0.05$ compared with CBDL.